

Proton structure using light-front dynamics

Emanuel Ydrefors

Institute of Modern Physics, China

Collaborators: T. Frederico (ITA) and V. A. Karmanov (Lebedev Institute), and the group of X. Zhao (IMP)

Reference: PRD 104, 114012 (2021)

Frontiers in Nuclear Structure Theory
(KTH and Online)
May 23-25, 2022

- Introduction
 - Motivation
 - Light-front (LF) dynamics
- Relativistic studies of three-body system with contact interactions
- Effective model for the proton on the LF
- Results for proton distributions
- Conclusion

Motivation: Importance of proton structure for nuclear physics

- The proton used as a probe in nuclear physics, so important to know its structure.
- In calculations of e.g. cross sections for neutrino-nucleus scattering it is needed the electromagnetic and weak form factors of the nucleons.
- The nuclear force is a remnant of the strong force (described by QCD) between quarks and gluons, i.e. knowledge about the properties of the QCD at low energy is important to understand the nuclear force from first principles.

- In hadron physics, one important but difficult remaining challenge is to describe the dynamics and structure of the proton in terms of its basic constituents (quarks and gluons).
- The structure of a hadron (e.g. a proton, pion, etc) in momentum space can be studied through various physical quantities, e.g.
 - Electromagnetic form factors
 - The parton distribution function (PDF). I.e., the probability distribution for a quark to have a given fraction x of the total longitudinal momentum $P^+ = P^0 + P^3$.
 - Transverse momentum distributions, giving also dependence on the transverse momentum of the quark.
- As will be explained in the following, the above quantities and others can be accessed through the so-called proton light-front wave function, which is the analog of the wave function in NR QM.

- Dynamical system is characterized by ten fundamental quantities, i.e. energy, momentum, angular momentum and boosts.
- Conventional form (instant form): dynamical variables refer to physical conditions at some instant time, e.g. $x^0 = 0$. But, as pointed out by Dirac, other choices are possible. In the Light-front (LF) dynamics refer to conditions on a front $x^+ = t + z = 0$. So, commutation relations defined at equal LF time ($x^+ = 0$).
- LF variables: $x^\pm = t \pm z$ and similarly for the momenta.
- After integration over relative momentum k^- and putting $x^+ = 0$, the four-dimensional space reduced to a three-dimensional one (k^+, \vec{k}_\perp).

Light-front Dynamics (LFD) turns out to be convenient for description of, in particular, relativistic bound states:

- It allows a Fock space expansion of a state vector in terms of contribution with well-defined particle-number. For example, for a three-body system:

$$|p\rangle = |n=3\rangle + |n=4\rangle + \dots \quad (1)$$

where each term has an associated boost-invariant wave function Ψ_n with probability

$$P_n = \left\{ \prod_{i=1}^n \int \frac{d^2 k_{i\perp}}{(2\pi)^2} \int_0^1 dx_i \right\} \delta\left(1 - \sum_{i=1}^n x_i\right) \delta\left(\sum_{i=1}^n \vec{k}_{i\perp}\right) |\Psi_n(x_1, \vec{k}_{1\perp}, x_2, \vec{k}_{2\perp}, \dots)|^2 \quad (2)$$

In Eq. (1), the leading contribution is referred to as valence component.

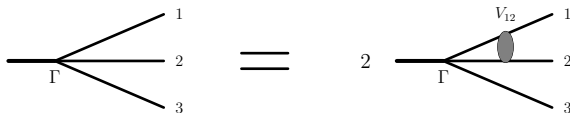
- Using the Fock space expansion one can derive a Schroedinger like equation of the form ($P_\perp = 0$)

$$H_{LC}|\Psi\rangle = M^2|\Psi\rangle, \quad H_{LC} = P^+ P^-, \quad (3)$$

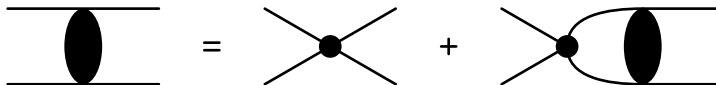
with P^+ diagonal and P^- a functional. But, in practice Fock-expansion has to be truncated to finite order.

- In the long-term perspective, to create a fully dynamical model for the proton in Minkowski space.
- It will then give direct access to observables defined on the so-called light-front hyperplane.
- As a first step, Fock basis truncated to valence order, i.e. proton is uud , and spin degree-of-freedom not included.
- Quark-diquark model with dynamical diquark in s-wave channel interacting through contact interaction between two of the quarks. In that sense it is an effective low-energy model.
- The proton structure will be explored through momentum distribution and its so-called Ioffe-time representation of the wave function.

Three-body model



- Three spinless particles of mass m . Spectator + pair of interacting particles. Factor of two due to symmetry of wave function with respect to exchange of the particles.



- In the present work a zero-range interaction with four-leg-vertex $i\lambda$ used. Then, for the two-body amplitude (see figure)

$$i\mathcal{F}(M_{12}^2) = i\lambda + (i\lambda)^2 \mathcal{B} + (i\lambda)^3 \mathcal{B}^2 + \dots = \frac{1}{(i\lambda)^{-1} - \mathcal{B}(M_{12}^2)} \quad (4)$$

with the bubble diagram

$$\mathcal{B}(M_{12}^2) = \int \frac{d^4k}{(2\pi)^4} \frac{i}{(k^2 - m^2 + i\epsilon)} \frac{i}{[(k - P)^2 - m^2 + i\epsilon]} \quad (5)$$

- where $M_{12}^2 = P^2$ with P total four-momentum of two-body system.

- However, the integral entering definition of \mathcal{B} logarithmic divergent. We regularize and renormalize the two-body scattering amplitude by fixing the scattering length at the continuum threshold

$$\frac{1}{16\pi m} \mathcal{F}(4m^2) = -a, \quad (6)$$

giving

$$\mathcal{F}(M_{12}^2) = \frac{1}{i[\mathcal{B}(4m^2) - \mathcal{B}(M_{12}^2)] - \frac{1}{16\pi m a}}. \quad (7)$$

- For $a > 0$ it is equivalent to fixing a two-body mass M_2 (pole of scattering amplitude) where

$$a = \frac{\pi y'_{M_2}}{2m \arctan(y'_{M_2})}, \quad y'_{M_2} = \frac{M_2}{\sqrt{4m^2 - M_2^2}}. \quad (8)$$

Three-body Faddeev-Bethe-Salpeter equation with zero interaction

- We consider the case of three spinless bosons of equal mass. The structure contained in the so-called Bethe-Salpeter amplitude given by

$$i\Phi(q_1, q_2, q_3) = i^3 \frac{v(q_1) + v(q_2) + v(q_3)}{(q_1^2 - m^2 + i\epsilon)(q_2^2 - m^2 + i\epsilon)(q_3^2 - m^2 + i\epsilon)}. \quad (9)$$

- Here $v(q)$ obey the Faddeev-Bethe-Salpeter (FBS) equation [1]:

$$v(q) = 2i\mathcal{F}(M_{12}^2) \int \frac{d^4k}{(2\pi)^4} \frac{i}{k^2 - m^2 + i\epsilon} \frac{i}{(p - q - k)^2 - m^2 + i\epsilon} v(k) \quad (10)$$

- A pole fixed in $\mathcal{F}(M_{12}^2)$, corresponding either to a two-body bound ($a > 0$) or virtual ($a < 0$) state, where a denotes the scattering length
- $\mathcal{F}(M_{12}^2)$, where $M_{12}^2 = (p - q)^2$, given by

$$\mathcal{F}(M_{12}^2) = \frac{\Theta(-M_{12}^2)}{\frac{1}{16\pi^2 y} \log \frac{1+y}{1-y} - \frac{1}{16\pi ma}} + \frac{\Theta(M_{12}^2) \Theta(4m^2 - M_{12}^2)}{\frac{1}{8\pi^2 y'} \arctan y' - \frac{1}{16\pi ma}} + \frac{\Theta(M_{12}^2 - 4m^2)}{\frac{y''}{16\pi^2} \log \frac{1+y''}{1-y''} - \frac{1}{16\pi ma} - \frac{iy''}{16\pi}}, \quad (11)$$

- The FBS equation was recently solved including the infinite number of Fock components in Euclidean [2] and Minkowski [3] space.

[1] T. Frederico, PLB 282 (1992) 409

[2] E. Ydrefors et al, PLB 770 (2017) 131

[3] E. Ydrefors et al, PLB 791 (2019) 276

Valence LF equation

- After the LF projection, i.e. introducing $k_{\pm} = k_0 \pm k_z$ and integrating over k_- , one obtains the valence three-body LF equation [1, 2]:

$$\Gamma(x, k_{\perp}) = \frac{\mathcal{F}(M_{12}^2)}{(2\pi)^3} \int_0^{1-x} \frac{dx'}{x'(1-x-x')} \int_0^{\infty} \frac{d^2 k'_{\perp}}{M_0^2 - M_N^2} \Lambda(M_0^2) \Gamma(x', k'_{\perp}) \quad (12)$$

with the squared free three-body mass

$$M_0^2 = (k'_{\perp}{}^2 + m^2)/x' + (k_{\perp}^2 + m^2)/x + ((k'_{\perp} + k_{\perp})^2 + m^2)/(1-x-x') \quad (13)$$

- Form factor introduced via subtraction, i.e.

$$[M_0^2 - M_N^2]^{-1} - [M_0^2 + \mu^2]^{-1} = \Lambda(M_0^2) [M_0^2 - M_N^2]^{-1} \rightarrow \Lambda(M_0^2) = [M_0^2 + \mu^2]^{-1} [M_N + \mu^2], \quad (14)$$

where μ is a cut-off mass.

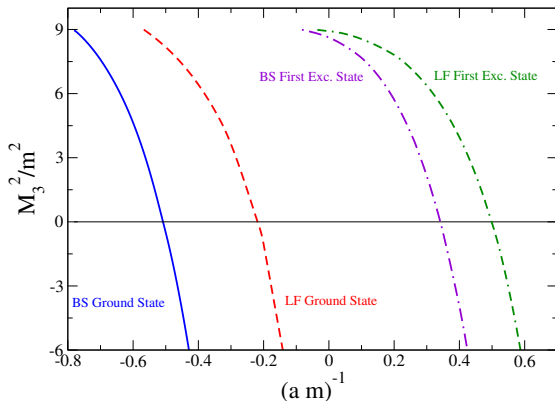
- The form factor eliminates the unphysical ground state, with $M_N^2 < 0$, and also lead to an infrared enhancement. Essentially, it removes contributions corresponding to high momenta \leftrightarrow short distances.
- The three-body valence LF wave function is given by

$$\Psi_3(x_1, \vec{k}_{1\perp}, x_2, \vec{k}_{2\perp}, x_3, \vec{k}_{3\perp}) = \frac{\Gamma(x_1, \vec{k}_{1\perp}) + \Gamma(x_2, \vec{k}_{2\perp}) + \Gamma(x_3, \vec{k}_{3\perp})}{\sqrt{x_1 x_2 x_3} (M_N^2 - M_0^2(x_1, \vec{k}_{1\perp}, x_2, \vec{k}_{2\perp}, x_3, \vec{k}_{3\perp}))}, \quad (15)$$

where due to momentum conservation: $x_3 = 1 - x_1 - x_2$ and $\vec{k}_{3\perp} = -\vec{k}_{1\perp} - \vec{k}_{2\perp}$.

[1] J. Carbonell and V.A. Karmanov, PRC 67 (2003) 037001

[2] T. Frederico, PLB 282 (1992) 409



- As studied in PLB 770 (2017) 131, for $\Lambda = 1$, it exists a lower-lying unphysical solution with $M_N^2 < 0$. This is the relativistic analog of the well-known Thomas collapse. But, contrary to the non-relativistic case the unphysical state has a finite energy, due to a short-range repulsion of purely relativistic origin.
- Difference between valence LF result and full BS solution, due to a contribution coming from an infinite number of diagrams involving anti-particles, which can be interpreted as an effective three-body force of relativistic origin.

- The valence contribution to the Dirac form factor is obtained from the matrix element of γ^+ . In the frame $q^+ = 0$ and $q^2 = -Q^2 = -q_\perp^2$ it is given by

$$F_1(Q^2) = \left\{ \prod_{i=1}^3 \int \frac{d^2 k_{i\perp}}{(2\pi)^2} \int_0^1 dx_i \right\} \delta \left(1 - \sum_{i=1}^3 x_i \right) \delta \left(\sum_{i=1}^3 \vec{k}_{i\perp}^f \right) \Psi_3^\dagger(x_1, \vec{k}_{1\perp}^f, \dots) \Psi_3(x_1, \vec{k}_{1\perp}^i, \dots), \quad (16)$$

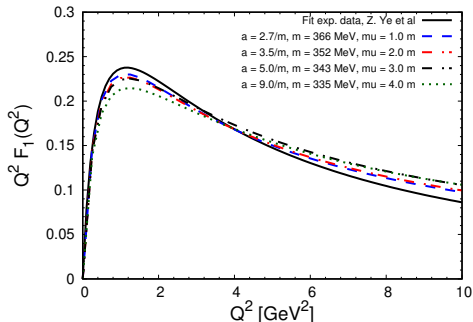
where $Q^2 = \vec{q}_\perp \cdot \vec{q}_\perp$ and the magnitudes of the momenta read

$$|\vec{k}_{i\perp}^{f(i)}|^2 = |\vec{k}_{i\perp} \pm \frac{\vec{q}_\perp}{2} x_i|^2 = \vec{k}_{i\perp}^2 + \frac{Q^2}{4} x_i^2 \pm \vec{k}_{i\perp} \cdot \vec{q}_\perp x_i \quad (i = 1, 2), \quad (17)$$

and

$$|\vec{k}_{3\perp}^{f(i)}|^2 = \left| \pm \frac{\vec{q}_\perp}{2} (x_3 - 1) - \vec{k}_{1\perp} - \vec{k}_{2\perp} \right|^2 = \quad (18)$$

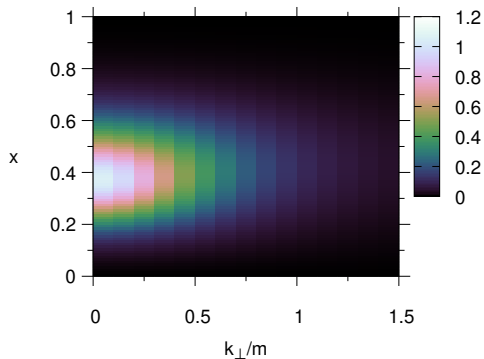
$$(1 - x_3)^2 \frac{Q^2}{4} \pm (1 - x_3) \vec{q}_\perp \cdot (\vec{k}_{1\perp} + \vec{k}_{2\perp}) + (\vec{k}_{1\perp} + \vec{k}_{2\perp})^2.$$



- In figure $Q^2 F_1(Q^2)$ for different values of a and μ compared with fit to exp. data by Z. Ye et al [1].
- Best agreement obtained for $a \approx 1.46$ fm and $\mu = m = 366$ MeV, and this parameters will be used in the following.
- Fair agreement with exp. data for $Q^2 < 5$ GeV² but for larger values of Q^2 they deviate, presumably due to lack of a finite-range interaction.

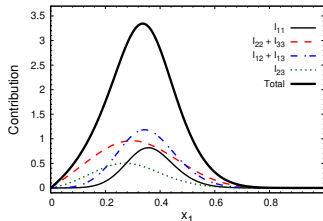
Z. Ye et al, PLB 777 (2018) 8.

Results for the vertex function



- The proton structure contained in the vertex function $\Gamma(x, k_\perp)$. Concentrated at small k_\perp and $x \sim 1/3$.

Parton distribution function at model scale



- The single parton distribution function (PDF), is the integrand of the form factor at $Q^2 = 0$, i.e.

$$f_1(x_1) = \frac{1}{(2\pi)^6} \int_0^{1-x_1} dx_2 \int d^2k_{1\perp} d^2k_{2\perp} |\Psi_3(x_1, \vec{k}_{1\perp}, x_2, \vec{k}_{2\perp}, x_3, \vec{k}_{3\perp})|^2 = I_{11} + I_{22} + I_{33} + I_{12} + I_{13} + I_{23}. \quad (19)$$

with the Faddeev contributions

$$I_{ii} = \frac{1}{(2\pi)^6} \int_0^{1-x_1} dx_2 \int d^2k_{1\perp} d^2k_{2\perp} \frac{\Gamma^2(x_i, \vec{k}_{i\perp})}{x_1 x_2 x_3 (M_N^2 - M_0^2(x_1, \vec{k}_{1\perp}, x_2, \vec{k}_{2\perp}, x_3, \vec{k}_{3\perp}))^2}$$

$$I_{ij} = \frac{2}{(2\pi)^6} \int_0^{1-x_1} dx_2 \int d^2k_{1\perp} d^2k_{2\perp} \frac{\Gamma(x_i, \vec{k}_{i\perp}) \Gamma(x_j, \vec{k}_{j\perp})}{x_1 x_2 x_3 (M_N^2 - M_0^2(x_1, \vec{k}_{1\perp}, x_2, \vec{k}_{2\perp}, x_3, \vec{k}_{3\perp}))^2}; \quad i \neq j. \quad (20)$$

- The PDF at model scale is peaked around $x = 1/3$ and quite narrow. None of the Faddeev contributions are negligible.

- Information about the proton PDF can be obtained from e.g. deep inelastic scattering

$$e + p \longrightarrow e + X, \quad (21)$$

where X is undetected.

- The differential cross section is of the form

$$\frac{d\sigma}{dx dQ^2} \sim \sum_{i=q,g} \int_x^1 \frac{dz}{z} C_i(z, Q^2) f_{i/p}(x/z, Q^2), \quad (22)$$

with the sum running over active quark flavors and gluon and $f_{i/p}$ the corresponding PDF. The coefficient functions C_i is obtained from perturbative QCD.

- For the comparison with other frameworks and/or experimental data the PDF should be evolved from the model scale to a higher scale.
- This is done by using the DGLAP equation

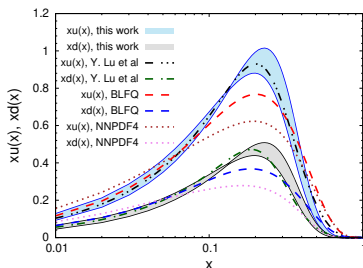
$$\frac{dq}{d\log Q^2} = \frac{\alpha_s(Q^2)}{2\pi} \int_x^1 P(x/y, \alpha_s(Q)^2) q(y, Q^2) \quad (23)$$

- We will use the effective coupling (EPJC 80 (2020) 1064):

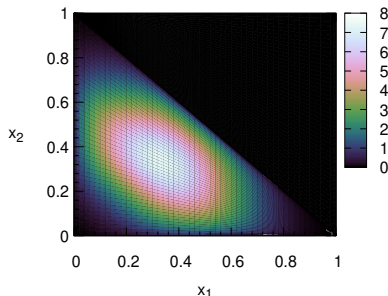
$$\alpha_s(k^2) = \frac{\gamma_m \pi}{\log[\mathcal{K}^2(k^2)/\Lambda_{QCD}^2]}, \quad \mathcal{K}^2(y) = (a_0^2 + a_1 y + y^2)/(b_0 + y) \quad (24)$$

- The initial scale is given by the hadron scale $Q_0 = 0.330 \pm 0.03$ GeV.

Proton PDF at $Q = 3.097$ GeV



- Colored areas: Computed u and d-quark xpdfs at $Q = 3.097$ GeV with the areas corresponding to the uncertainty in initial scale $Q_0 = 0.330 \pm 0.03$ GeV.
- Dash-dotted lines: Results from quark-diquark by Y. Lu et al [1]. Reasonable agreement. Disagreement at large x probably due to the use of contact interaction in our model.
- Dashed-lines: Basis Light-front Quantization (BLFQ) [1] but evolved using same framework as in this work. Only good agreement for small x .
- Dotted lines: Results from the NNPDF 4.0 global fit. None of the models agree well with these results.
- A few remarks:
 - Model of this work and the one by Y. Lu et al, are both quark-diquark models, but the latter one has also axial-vector diquark and a more realistic quark-quark interaction.
 - The BLFQ which is a Hamiltonian approach include (at least effectively) confinement, which is lacking in the two other models.



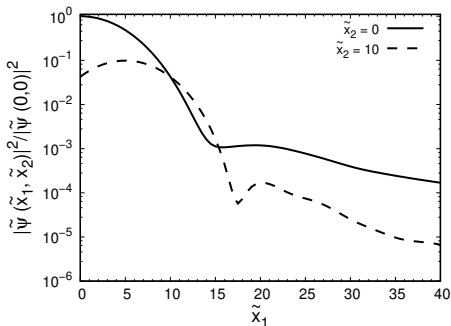
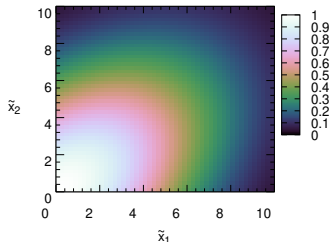
- The distribution amplitude is defined as

$$\phi(x_1, x_2) = \int d^2 k_{1\perp} d^2 k_{2\perp} \Psi_3(x_1, \vec{k}_{1\perp}, x_2, \vec{k}_{2\perp}, x_3, \vec{k}_{3\perp}). \quad (25)$$

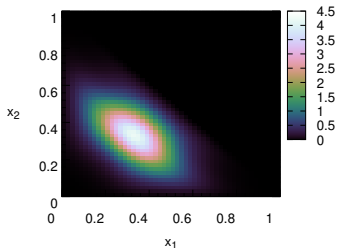
- It shows the dependence of the wave function on the momentum fractions for the case when the quarks share the same position.
- Triangular shape due to $x_1 + x_2 \leq 1$. Distribution centered around $x_1 = x_2 = 1/3$ but quite wide.

- Alternatively, the proton can be studied in coordinate space, in terms of the transverse position ($\vec{b}_{i\perp}$) and the Ioffe-time $\tilde{x}_i = b_i^- p^+$. The image of the proton is then obtained through the Fourier transform of the proton LF wave function.
- For simplicity, we consider here the case $\vec{b}_{1\perp} = \vec{b}_{2\perp} = \vec{0}_\perp$, and then one has

$$\Phi(\tilde{x}_1, \tilde{x}_2) \equiv \tilde{\Psi}_3(\tilde{x}_1, \vec{0}_\perp, \tilde{x}_2, \vec{0}_\perp) = \int_0^1 dx_1 e^{i\tilde{x}_1 x_1} \int_0^{1-x_1} dx_2 e^{i\tilde{x}_2 x_2} \phi(x_1, x_2), \quad (26)$$



- For $\tilde{x}_1 \geq 10$ a rather dramatic decrease of the amplitude is seen.
- An exponential damping is seen with respect to the relative distance in Ioffe-time between the two quarks. We expect this damping to be even more significant if confinement is incorporated, as its more effective at large distances.

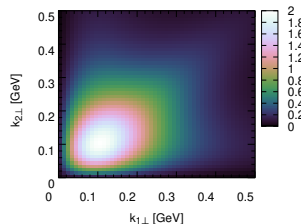
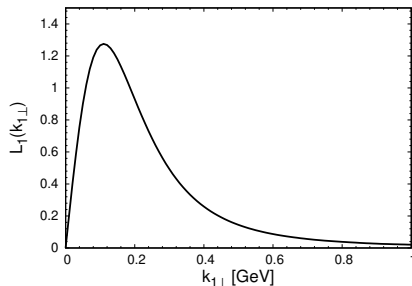


- The valence double parton distribution function (DPDF) is given by

$$D_3(x_1, x_2; \vec{\eta}_\perp) = \frac{1}{(2\pi)^6} \int d^2k_{1\perp} d^2k_{2\perp} \times \Psi_3^\dagger(x_1, \vec{k}_{1\perp} + \vec{\eta}_\perp; x_2, \vec{k}_{2\perp} - \vec{\eta}_\perp; x_3, \vec{k}_{3\perp}) \Psi_3(x_1, \vec{k}_{1\perp}; x_2, \vec{k}_{2\perp}; x_3, \vec{k}_{3\perp}). \quad (27)$$

- Fourier transform of $D_3(x_1, x_2, \vec{\eta}_\perp)$ in $\vec{\eta}_\perp$ gives the probability of finding the quarks 1 and 2 with momentum fractions x_1 and x_2 at a relative distance \vec{y}_\perp within the proton.
- In the figure is shown results for $\eta_\perp = 0$, showing a distribution centered around $x_1 = x_2 = 1/3$.

Transverse momentum densities



- The single quark transverse momentum density in the forward limit and integrated in the longitudinal momentum is associated with the probability density to find a quark with momentum k_{\perp} .
- It can be computed as:

$$L_1(k_{1\perp}) = \frac{k_{1\perp}}{(2\pi)^6} \int_0^1 dx_1 \int_0^{1-x_1} dx_2 \int_0^{2\pi} d\theta_1 \int d^2k_{2\perp} |\psi_3(x_1, \vec{k}_{1\perp}, x_2, \vec{k}_{2\perp}, x_3, \vec{k}_{3\perp})|^2. \quad (28)$$

- Two-quark one:

$$L_2(k_{1\perp}, k_{2\perp}) = \frac{k_{1\perp} k_{2\perp}}{(2\pi)^6} \int_0^1 dx_1 \int_0^{1-x_1} dx_2 \int_0^{2\pi} d\theta_1 \int_0^{2\pi} d\theta_2 |\psi_3(x_1, \vec{k}_{1\perp}, x_2, \vec{k}_{2\perp}, x_3, \vec{k}_{3\perp})|^2. \quad (29)$$

- The three-body FBS equation with zero-range interaction, including the infinite number of Fock components, was solved by direct integration in Minkowski space in Ref. [1]. However, the solution was quite difficult from numerical point of view.
- However, like in the two-body case, the Nakanishi integral representation be used for vertex function:

$$v(q;p) = \int_{-4/3}^{2/3} dz \int_0^\infty \frac{d\gamma g(\gamma, z)}{\gamma - k^2 - (p \cdot q)z - i\epsilon} \quad (30)$$

- For the two-body scattering amplitude

$$\mathcal{F}(M_{12}^2) = \int_{4m^2}^\infty d\gamma \frac{\rho(\gamma)}{M_{12}^2 - \gamma + i\epsilon} \quad (31)$$

with the spectral function

$$\rho(\gamma) = -\frac{\theta(s - 4m^2)}{16\pi^2} \frac{y''}{\left(\frac{y''}{16\pi^2} \log \frac{1+y''}{1-y''} - \frac{1}{16\pi m a}\right)^2 + \left(\frac{y''}{16\pi}\right)^2} \quad (32)$$

- Construction of the integral equation for $g(\gamma, z)$ and its solution is under development.
- Observables could then be computed including all the infinite number of Fock components.

[1] E. Ydrefors et al, PLB 791 (2019) 276

- We have, in this work, studied the proton in a simple but fully dynamical valence LF model based on a zero-range interaction.
- The model is based on the concept of a strongly interacting scalar diquark.
- We have studied the structure of the proton by computing the LF wave function in its Ioffe-time representation and also momentum distributions.
- However, the model is rather crude since e.g. the spin degree of freedom hasn't been included yet. But is a first step towards studying the proton directly in Minkowski space.
- Future plans:
 - Generalization to the infinite set of Fock components (The Faddeev-Bethe-Salpeter equation solved in PLB 791 (2019) 276)
 - Implementation of a more realistic interaction (gluon exchange)
 - Inclusion of spin degree of freedom